Numerical Accuracy Case Studies: 2D Rimless Spoked Wheel and a 3D Passive-Dynamic Model of Walking

Michael J. Coleman Andy Ruina Anindya Chatterjee[1]
Department of Theoretical and Applied Mechanics
Cornell University, Ithaca, NY 14853-7501 USA

revised December 14, 2000

Draft: not for publication

[1]current address: Indian Institute of Science, Bangalore 560 012, INDIA

Abstract

We report on the estimates of the accuracy of standard numerical methods used to study the motions and stability of two systems with intermittent dynamics: (1) a 2D rigid rimless spoked wheel, or regular polygon, rolling downhill and (2) a 3D passive-dynamic walking machine. In the first case, solutions are known analytically so both the numerical result and error estimates can be checked. The eigenvalue error is about 1×10^{-10}. The same numerical and error estimation procedures are used for the second case where no analytical solution is known. The eigenvalue error is about 1×10^{-7}. The overall error estimation approach is similar to those in [1, 2, 3, 4, 5].

1 2D Rimless Spoked Wheel Rolling Downhill

We summarize here the mathematical formulation of the problem. The details of equation derivation and their solutions are in Coleman [6]. The configuration of the wheel is shown in Figure 1.

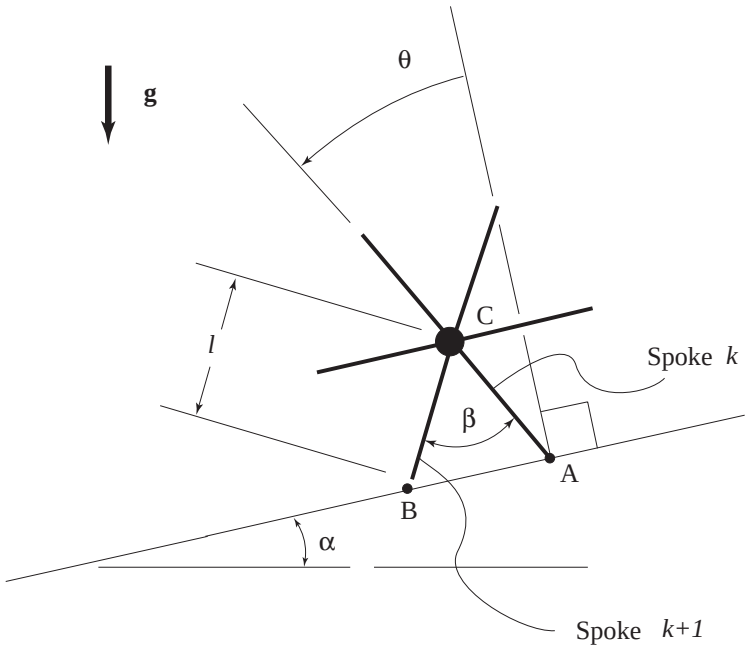

Figure 1: 2D rigid body model: a rimless spoked wheel of mass m, moment of inertia about the center of mass I_C, and n evenly spaced spokes of uniform mass and length l rolls down a slope of angle α. The orientation of the wheel is given by angle θ and its angular rate by $\dot{\theta}$. The angle between the spokes is $\beta = 2\pi/n$.

1.1 Governing Equations

The state vector describing the phase space is $\mathbf{q} = (\theta, y)$, where $y = \dot{\theta}$.

1. The first order system of differential equations governing the motion between collisions is:

$$\begin{aligned} \dot{\theta} &= y \\ \dot{y} &= \lambda^2 \sin(\theta + \alpha). \end{aligned} \tag{1}$$

2. The termination condition for detecting a downhill spoke collision is:

$$\theta = \pi/n. \tag{2}$$

3. The jump transition rule at spoke collision is:

$$(\theta, y) \mapsto (-\theta, \mu y), \qquad \theta = \pi/n. \tag{3}$$

λ, α, and n are constants, where $0 < \lambda \leq 1$, and

$$\mu = 1 + \lambda^2(\cos(\frac{2\pi}{n}) - 1), \qquad 0 \leq \mu < 1. \tag{4}$$

1.2 Poincaré section, Return Map, Fixed Points, and Stability

We study this system by sampling the phase space at the points of discontinuity, the collisions, where we know the pitch angle of the wheel to be $\theta = \frac{\pi}{n}$. We then write a map from one point just after a collision, to the next, as the difference equation

$$\mathbf{q}_{k+1} = \mathbf{f}(\mathbf{q}_k), \tag{5}$$

where we call $\mathbf{f}$ the *return map* (or Poincaré map) and $\mathbf{q}_k$ is the state vector of the system at the start of a cycle, just after the k_{th} spoke collision.

In this problem, $\mathbf{f}$ can be found explicitly as

$$\left\{ \begin{array}{c} \theta_{k+1} \\ y_{k+1} \end{array} \right\} = \mathbf{f}(\mathbf{q}_k) = \left\{ \begin{array}{c} f_1(\theta_k, y_k) \\ f_2(\theta_k, y_k) \end{array} \right\} = \left\{ \begin{array}{c} -\frac{\pi}{n} \\ \mu\sqrt{y_k^2 + 2\lambda^2(\cos(\alpha - \frac{\pi}{n}) - \cos(\alpha + \frac{\pi}{n}))} \end{array} \right\}. \tag{6}$$

Any $\mathbf{q}^*$ for which $\mathbf{f}(\mathbf{q}^*) = \mathbf{q}^*$ is a fixed point. The fixed point of the return map is:

$$\left\{ \begin{array}{c} \theta^* \equiv \theta^*(n) \\ y^* \equiv y^*(\alpha, n, \lambda^2) \end{array} \right\} = \left\{ \begin{array}{c} -\frac{\pi}{n} \\ \sqrt{\frac{4\mu^2\lambda^2 \sin\frac{\pi}{n} \sin\alpha}{1-\mu^2}} \end{array} \right\} \tag{7}$$

The Jacobian of $\mathbf{f}$ evaluated at the fixed point can be computed explicitly as:

$$\mathbf{J}(\mathbf{q}^*) = \left[\begin{array}{cc} 0 & 0 \\ \frac{-\mu\lambda^2 \sin(\alpha - \frac{\pi}{n})}{2\sqrt{\frac{\lambda^2 \sin\frac{\pi}{n} \sin\alpha}{1-\mu^2}}} & \mu^2 \end{array} \right] \tag{8}$$

The two eigenvalues are $\sigma_1 = 0$ and $\sigma_2 = \mu^2$.

For the numerical analysis, we take the wheel parameters to be

$$\begin{aligned} n &= 6, \\ \lambda^2 &= 2/3, \text{ and} \\ \alpha &= 0.2 \end{aligned} \tag{9}$$

The fixed point angular rate, from the algebra above, is

$$y^* = \sqrt{\frac{4\mu^2\lambda^2 \sin\frac{\pi}{n} \sin\alpha}{1-\mu^2}} = 0.4603411266094583 \tag{10}$$

and the stability eigenvalues are:

$$\begin{aligned} \sigma_1 &= 0 \\ \sigma_2 &= \mu^2 = 4/9 = 0.4444444444444\overline{4}. \end{aligned} \tag{11}$$

2 Numerical Analysis and Error Estimation

We now estimate the error in the numerical calculation of fixed points and stability eigenvalues *with* and *without* reference to a closed form solution. In order to investigate the error in computing the stability eigenvalues for a map evaluated at a fixed point, we first determine the accuracy of one numerical map iteration. Then, using the integration step size that approximately minimizes the map evaluation error, we find a fixed point of the map. Finally, we compute components of the Jacobian matrix which requires 2 map evaluations slightly perturbed from the fixed point, one for each of the matrix columns.

2.1 Map Evaluation Error

We carry out one map iteration numerically as follows: (**1**) we integrate the system of differential equations forward from the state of the system just after a collision using a constant step size 4^{th} order Runge-Kutta scheme written in MATLAB® combined with Henon's [7] method to detect collisions and return the state just before the next spoke collision; and, (**2**) a matrix multiplication applies the transition conditions at impact, taking the state of the system just before a spoke collision to just after; *i.e.*, Equation 3 can be accomplished by a matrix multiplication.

We would like to know what Runge-Kutta step size h we should select to minimize the errors in finding a fixed point and the stability eigenvalue. We proceed assuming that we do not know the true answer for either.

To do this, we study how $\mathbf{q}_{k+1} = \mathbf{f}(\mathbf{q}_k)$ varies with the step size. The steps for investigating how the error in calculating a desired quantity, say x, scales with the desired integration step size are as follows:

1. Integrate forward from some initial condition x_0 near the eventual fixed point over one map iteration to $x_1 = f(x_0)$ at some fixed integration time step h_j. (Note: the last time step is not h_j but smaller, since it is chosen to make the collision detection condition be satisfied to some accuracy.)

2. Integrate forward from the same initial condition over one map iteration for a range of step sizes h_1, $h_2 = Ch_1$, ..., $h_{j+1} = Ch_j$, ... or $h_j = C^{j-1}h_1$.

3. If the true answer is $\hat{x}_1$, then the absolute error for h_j is

$$\Delta_j = x_1(h_j) - \hat{x}_1. \tag{12}$$

4. By eliminating $\hat{x}_1$, form the difference in absolute error between calculations at successive step sizes as:

$$|\Delta_{j+1} - \Delta_j| = |x_1(h_{j+1}) - x_1(h_j)|; \tag{13}$$

If round-off errors are not significant, for 4^{th} order Runge-Kutta integration, we expect

$$\begin{aligned} \Delta_j &\approx Kh_j^4 \\ \Delta_{j+1} &\approx Kh_{j+1}^4 = KC^4h_j^4 \\ \Rightarrow (\Delta_{j+1} - \Delta_j) = x_1(h_{j+1}) - x_1(h_j) &\approx K(1-C^4)h_j^4 \qquad (14) \\ \Rightarrow \frac{(\Delta_{j+1} - \Delta_j)}{(1-C^4)} = \frac{x_1(h_{j+1}) - x_1(h_j)}{(1-C^4)} &\approx Kh_j^4. \qquad (15) \end{aligned}$$

5. Plot $\log_{10}(|x_1(h_{j+1}) - x_1(h_j)|/(1-C^4))$ versus $\log_{10}(h_j)$; such a plot should indicate the map iteration error and corresponding integration step size h_j, assuming negligible round-off error.

We investigate the integration error over one step near an estimate for a fixed point. In order to find a fixed point of the map $\mathbf{f}$, we integrate forward from some arbitrary initial condition $\mathbf{q}_k$ and find $\mathbf{q}_{k+1} = \mathbf{f}(\mathbf{q}_k)$, form the difference $\mathbf{g}(\mathbf{q}_k) = \mathbf{f}(\mathbf{q}_k) - \mathbf{q}_k = \mathbf{q}_{k+1} - \mathbf{q}_k$, and use Newton's method to reduce the difference to some acceptably small number, or *termination criterion*, ϵ_N near zero.

To start, we take arbitrarily the integration step size, the termination criterion for Newton's method, and Jacobian forward difference step size to be, respectively:

$$\begin{aligned} h &= 0.001, \\ \epsilon_N &= 1 \times 10^{-14}, \text{ and} \\ \delta &= 1 \times 10^{-7}. \end{aligned} \tag{16}$$

We get the fixed point

$$(\theta^*, y^*) = (-\pi/n, 0.46034112660946) \tag{17}$$

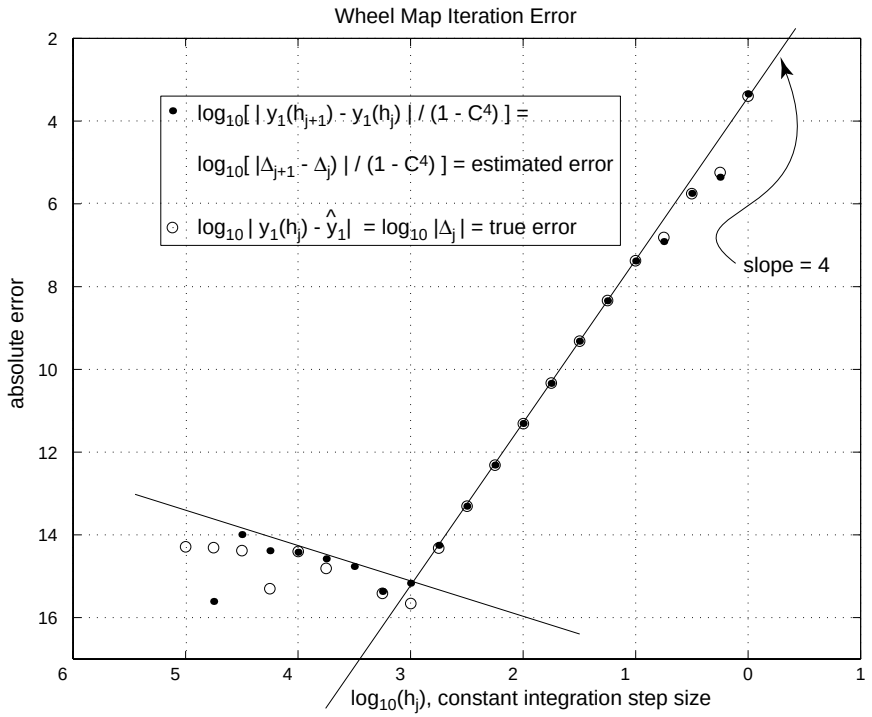

Figure 2: Absolute error in the angular rate y over one forward map iteration for $n = 6$, $\lambda^2 = 2/3$, and $\alpha = 0.2$ where $C = 10^{-1/4}$. Note that the truncation error has slope approximately equal to 4 as expected. The open circles denote the error with respect to one true map iterate $\hat{y}_1$ using Equation 6 and the solid circles denote the estimated error based on single map iterates calculated at successive step sizes.

which we use as our initial values (θ_0, y_0) for the step size convergence study. After one map iteration at a particular step size h_j, we obtain a new angular rate $y_1(h_j)$.

Following the procedure outlined above for error estimation, Figure 2 shows a $\log_{10} - \log_{10}$ plot of:

1. $|y_1(h_{j+1}) - y_1(h_j)/(1 - C^4)|$ vs. h_j where $C = 10^{-1/4}$ (represented by solid circles), and
2. $|y_1(h_{j+1}) - \hat{y}_1|$ vs. h_j (represented by open circles).

To get the most precise map iterate, based on the plot, we choose the step size we will use for the eigenvalue study to be (see Figure 2)

$$h = 10^{-3} = 0.001. \tag{18}$$

The truncation error between calculations at successive integration step size appears reasonably minimized at about

$$\Delta \approx 1 \times 10^{-15}. \tag{19}$$

below which there is no apparent gain in accuracy and round-off error becomes prominent. We use this value of Δ as the termination criterion for Newton's method, $\epsilon_N = 1 \times 10^{-15}$ (since the Jacobian involved is of order 1). Finally, using the integration step size and termination criterion suggested above, we find a fixed point. In summary, we have

$$\begin{aligned} h &= 0.001, \\ \epsilon_N &= 1 \times 10^{-15}, \\ y^* &= 0.460341126609458 \end{aligned} \tag{20}$$

We use this step size and fixed point for the subsequent stability and eigenvalue error analysis.

2.2 Stability Eigenvalue Error

We generate the Jacobian matrix of the map evaluated at the fixed point numerically via the method of centered differences where the truncation error is $O(\delta^2)$, or quadratic in the difference step size δ. Finding each column of the Jacobian involves two map iterations. We use the MATLAB® function `eig.m`[1] to compute the eigenvalues of the Jacobian.

One eigenvalue is exactly zero ($\sigma_1 = 0$), and, as mentioned previously, reflects the fact that the initially perturbed point might lie off the Poincaré section, but the next iterate will lie exactly on the Poincaré section. Thus, we concern ourselves with the error in computing the second eigenvalue σ_2 which governs stability of the wheel fixed point. We compute the error in σ_2 in the same manner as was done for the map iteration error.

Using the integration step size found above, $h = 0.001$, Figure 3 shows a $\log_{10} - \log_{10}$ plots of:

1. $|\sigma_2(\delta_{j+1}) - \sigma_2(\delta_j)/(1 - C^2)|$ vs. δ_j evaluated at the numerically determined fixed point $y^* = 0.460341126609456$ and with $C = 10^{-1/4}$ (represented by solid circles) and
2. $|\sigma_2(\delta_j) - \hat{\sigma}_2|$ vs. δ_j (represented by open circles).

The error in the stability eigenvalue between estimates at successive step sizes is reasonably minimized at about

$$\Delta(\delta) \approx 1 \times 10^{-10} \tag{21}$$

at a central difference step size of about

$$\delta \approx 1 \times 10^{-5}. \tag{22}$$

This procedure, then, lets us bound the error safely for the stability eigenvalue,

$$\sigma_2 = 0.4444444444 \pm 1 \times 10^{-10}. \tag{23}$$

Compared to the map iteration error plotted in Figure 2, the eigenvalue round-off errors are more significant due to the fact that one Jacobian calculation by centered differences involves 4 map iterations; plus, additional errors are incurred due to invoking MATLAB® 's `eig.m`.

As for the map iteration error analysis, if round-off errors are not significant in the eigenvalue calculations, we expect the errors in the eigenvalue σ_2 to scale with central difference step size as follows:

$$\begin{aligned}
\Delta_j &\approx K_\sigma \delta_j^2 \\
\Delta_{j+1} &\approx K_\sigma \delta_{j+1}^2 = K_\sigma C_\sigma^2 \delta_j^2 \\
\Rightarrow (\Delta_{j+1} - \Delta_j) = \sigma_2(\delta_{j+1}) - \sigma_2(\delta_j) &\approx K_\sigma (1 - C_\sigma^2) \delta_j^2 \qquad (24) \\
\Rightarrow \frac{(\Delta_{j+1} - \Delta_j)}{(1 - C_\sigma^2)} = \frac{\sigma_2(\delta_{j+1}) - \sigma_2(\delta_j)}{(1 - C_\sigma^2)} &\approx K_\sigma \delta_j^2. \qquad (25)
\end{aligned}$$

2.3 Comparison of Numerical to Exact Solutions

We summarize the analytical and numerical calculations for the wheel thus far in Table 1: (1) the numerically determined fixed point differs from the analytical solution (Equation 10) in the 16^{th} decimal place; and, (2) the numerically evaluated stability eigenvalue differs from the analytical solution (Equation 11) in the 11^{th} decimal place. In addition, at a fixed central difference step size of $\delta = 10^{-5}$, the stability eigenvalue differed at most in the 9_{th} decimal place with the true solution while varying the integration step size from $h = 1 \times 10^{-2}$ to $h = 1 \times 10^{-5}$.

[1] `eig.m` uses EISPACK, a library of Fortran 77 routines for computing eigenvalues and eigenvectors in numerical linear algebra.

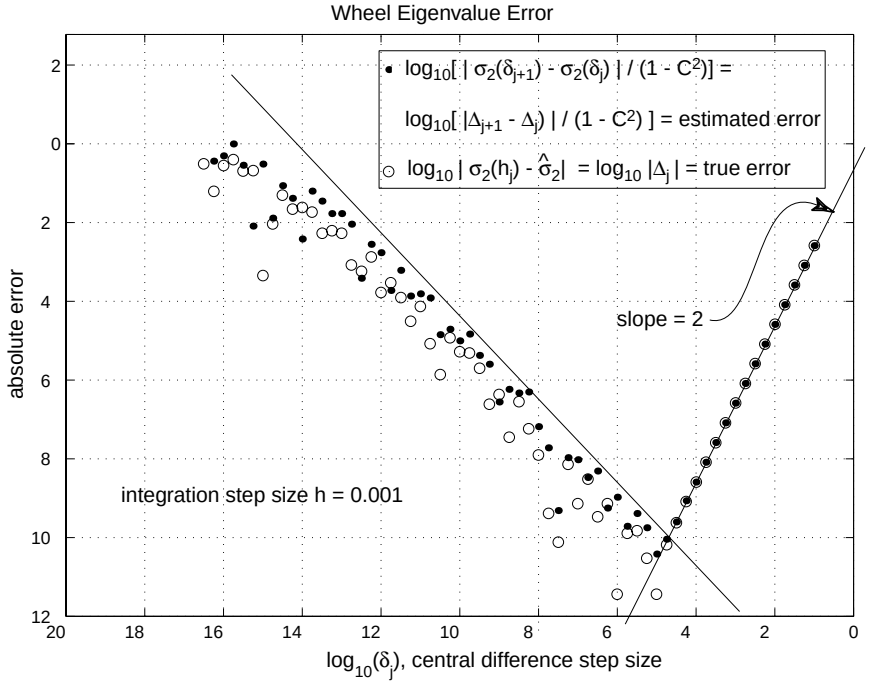

Figure 3: Absolute error in the stability eigenvalue σ_2 for $n = 6$, $\lambda^2 = 2/3$, and $\alpha = 0.2$ where $C_\sigma = 10^{-1/4}$. Note the quadratic convergence of the truncation error (slope 2 on the $\log_{10} - \log_{10}$ plot).The open circles denote the error with respect to the true eigenvalue $\hat{\sigma}_2$ using Equation 11 and the solid circles denote the estimated error based on eigenvalues calculated at successive central difference step sizes.

	y^*	σ_2
analytical	0.4603411266094583	4/9
numerical	0.4603411266094588	0.44444444444080
true error	5×10^{-16}	4.8×10^{-12}
estimated error	6.1×10^{-16}	6.2×10^{-11}

Table 1: Comparison of numerical and analytical calculations of the fixed point and stability eigenvalue for the 2D rimless wheel.

3 Error Analysis for the 3D Passive-Dynamic Walking Model

This analysis for the 2D rimless spoked wheel was carried out to better understand the errors involved in similar numerical procedures we apply to systems with intermittent dynamics where we *do not* know the true answer a priori, unlike the wheel. In particular, we apply these procedures in studying passive-dynamic walking mechanisms where we know neither the fixed points nor their stability analytically.

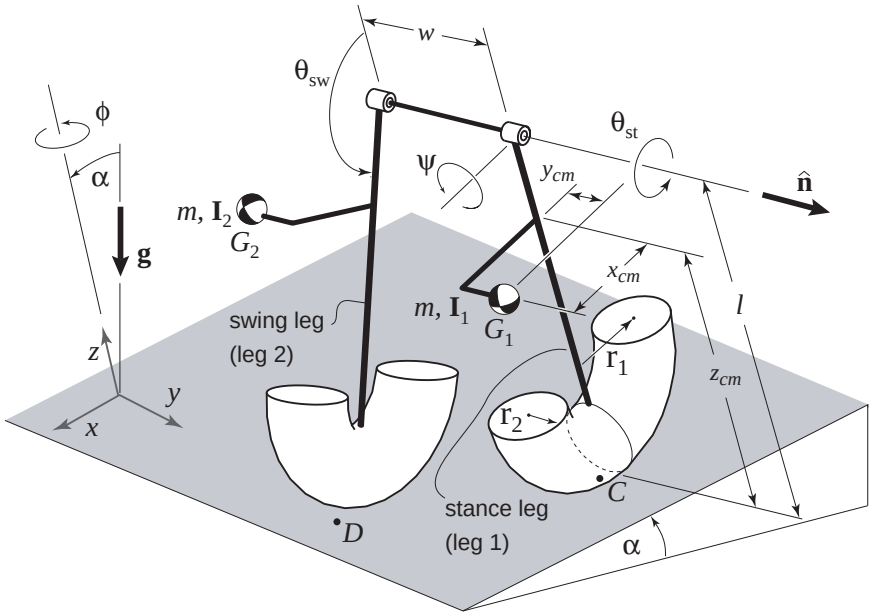

Figure 4: The 3D rigid body model. The parameters and state variables are described in [8].

We apply the approach described above in Section 2 for the wheel to the estimation of the error in maximum eigenvalue calculations for a 3D passive-dynamic straight-legged walking model shown in Fig. 4 (see [8, 9]). The physical parameters are: $I_{XX} = 0.1982$, $I_{YY} = 0.0186$, $I_{ZZ} = 0.1802$, $I_{XY} = 0.0071$, $I_{XZ} = -0.0023$, $I_{YZ} = 0.0573$, $\alpha = 0.0702$, $X_{cm} = 0$, $Y_{cm} = 0.6969$, and $Z_{cm} = 0.3137$, $W = 0.3624$, and $R_1 = 0.1236$ and $R_2 = 0$ (capital letters indicate nondimensional variables, I_{MN} are tensor components).

Following the procedure outlined above for error estimation, Figure 2 shows a $\log_{10} - \log_{10}$ plot of $|\theta_{\rm st}(h_{j+1}) - \theta_{\rm st}(h_j)/(1 - C^4)|$ vs. h_j where $C = 10^{-1/4}$. To get the most precise map iterate, based on the plot, we choose the step size we will use for the eigenvalue study to be (see Figure 5)

$$h = 3 \times 10^{-4} = 0.0003. \tag{26}$$

The truncation error between calculations at successive integration step size appears reasonably

minimized at about

$$\Delta \approx 1 \times 10^{-14} \tag{27}$$

below which there is no apparent gain in accuracy and round-off error becomes prominent. We use this value of Δ as the termination criterion for Newton's method, $\epsilon_N = 1 \times 10^{-14}$.

Finally, using the integration step size and termination criterion suggested above, we find a fixed point for the given parameters (see Table 2). We use this step size and fixed point for the subsequent stability and eigenvalue error analysis. The limit cycle period is $\tau^* = 1.00711403622059$ where $\dot{(\ )} = d(\ )/d\tau$ with τ the dimensionless time.

ϕ^*	0.09866765986740
ψ^*	-0.00924861067616
$\theta^*_{\rm st}$	-0.16016583495522
$\theta^*_{\rm sw}$	3.43583389038583
$\dot{\phi}^*$	-0.13220965510356
$\dot{\psi}^*$	-0.01990961987794
$\dot{\theta}^*_{\rm st}$	0.47124237466979
$\dot{\theta}^*_{\rm sw}$	-0.39255916866486

Table 2: Fixed point for the 3D walking model with the parameters cited in the text and an integration step size $h = 0.0003$.

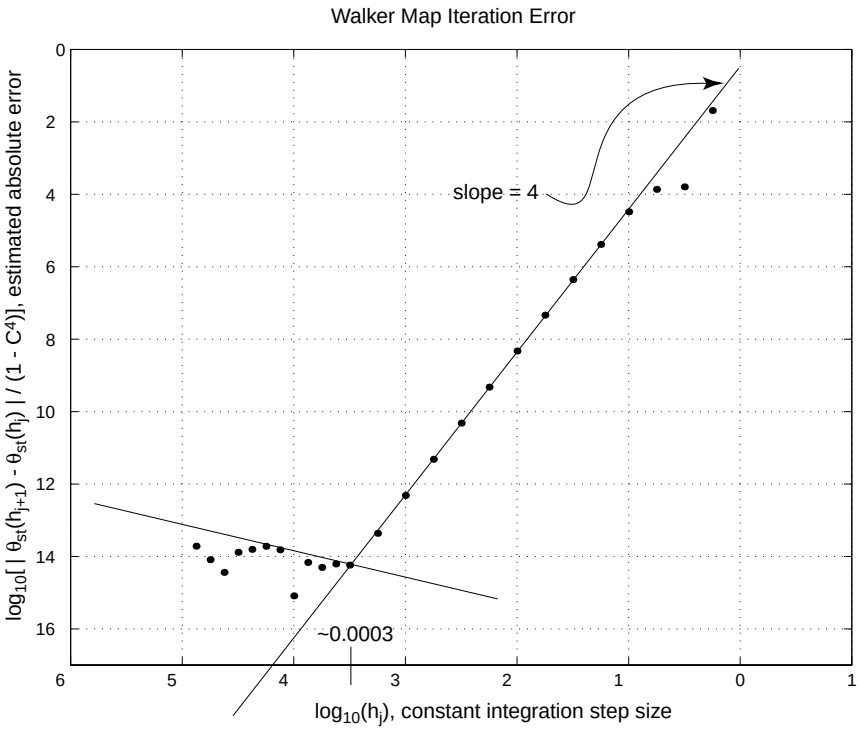

Figure 5: Error in the fixed point stance leg angle (for the 3D walking model of [9]) with the parameters cited in the text.

Figure 6 shows a $\log_{10} - \log_{10}$ plot of $|\ |\sigma(\delta_{j+1})|_{\max} - |\sigma(\delta_j)|_{\max}\ |$ vs. δ_j evaluated at the fixed point where we have used the integration step size found above, $h = 0.0003$. The error in the

stability eigenvalue between estimates at successive step sizes δ_j is reasonably minimized at about

$$\Delta(\delta) \approx 1 \times 10^{-7} \tag{28}$$

at a central difference step size of about

$$\delta \approx 1 \times 10^{-5}. \tag{29}$$

Compared to the map iteration error plotted in Figure 5, as for the wheel, the eigenvalue round-off errors are again more significant due to the fact that one Jacobian calculation by centered differences involves 16 map iterations. In addition, the round-off error for the walker is more significant than for the wheel since the number of operations to compute the Jacobian is greater by a factor of 4.

This procedure, then, lets us bound the error safely for the stability eigenvalue,

$$|\sigma|_{max} = 0.8391560 \pm 1 \times 10^{-7}. \tag{30}$$

In addition, at a fixed central difference step size of $\delta = 10^{-5}$, the maximum eigenvalue differed in the 8^{th} decimal place while varying the integration step size from $h = 10^{-3}$ to $h = 5.5 \times 10^{-4}$, for a number of values.

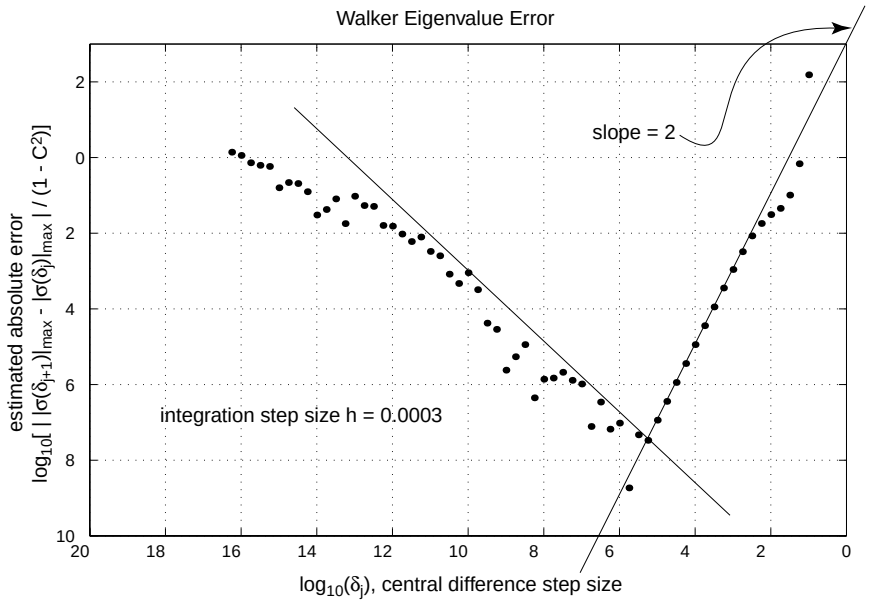

Figure 6: Absolute error in the maximum eigenvalue modulus eigenvalue (for the 3D walking model of [9]) for the parameters cited in the text. Again, note the quadratic convergence of the truncation error. The integration step size is $h = 0.0003$.

4 Acknowledgments

The authors thank David Cabrera and Mario Gomes for discussions on how to estimate numerical accuracy and for editing.

References

[1] D. Kahaner, C. Moler, and S. Nash. *Numerical Methods and Software.* Prentice Hall, Englewood Cliffs, New Jersey, 1989. pp. 17–35, pp. 272–330.

[2] F. B. Hildebrand. *Introduction to Numerical Analysis.* Dover, 2nd edition, 1974. pp. 1–39, pp. 240–303.

[3] M. K. Jain. *Numerical Solution of Differential Equations.* Wiley, New York, 2nd edition, 1984. pp. 1–93.

[4] E. Isaacson and H. B. Keller. *Analysis of Numerical Methods.* Dover, 1994. pp. 1–21, pp. 364–434.

[5] W. H. Press, B. P. Flannery, S. A. Teukolsky, and W. T. Vetterling. *Numerical Recipes: The Art of Scientific Computing.* Cambridge University Press, Cambridge, 1989. pp. 547–572.

[6] M. J. Coleman. *A Stability Study of a Three-dimensional Passive-dynamic Model of Human Gait.* PhD thesis, Cornell University, Ithaca, NY, 1998.

[7] M. Henon. On the numerical computation of Poincaré maps. *Physica 5D*, pages 412–414, 1982.

[8] M. J. Coleman and A. Ruina. An uncontrolled walking toy that cannot stand still. *Phys. Rev. Lett.*, 80(16):3658–3661, April 20 1998.

[9] K. Mombaur, M. J. Coleman, M. Garcia, and A. Ruina. Prediction of stable walking for a toy that cannot stand. In process, submitted to *Phys. Rev. Let.*, 2000.